A Stick-Slip Positioning Stage Robust to Load Variations

Yong Wang, Junhui Zhu, Ming Pang, Jun Luo, Shaorong Xie, Mei Liu, Lining Sun, Chao Zhou, Min Tan, Ji Ge, Yu Sun, *Senior Member, IEEE*, and Changhai Ru, *Member, IEEE*

***Abstract*—In stick-slip positioning, friction between the stick-slip surfaces plays a critical role in positioning accuracy. Positioning performance varies when the load to drive changes. In this paper, by using a form-closed cam, the driving unit is separated from the moving unit to eliminate load influence. The stage is capable of operating in either a stepping mode or a scanning mode. Numerical modeling was conducted to analyze the static and dynamic characteristics of the stage design. In experiments, a number of parameters were tested on the constructed stage, and positioning performance was measured via laser-doppler vibrometry. Experimental results demonstrate that in the stepping mode, the stage has a travel range of 2 mm with incremental step sizes ranging from 30 nm to 2.3 μm. In the scanning mode, the stage has a positioning resolution of 1.15 nm. The measured results also confirm that load variations on the stage have little influence on contact friction force and positioning performance.**

***Index Terms*—Flexible hinges, form-closed cam, load insensitive, precision positioning, stick-slip.**

Manuscript received April 17, 2015; revised November 02, 2015; accepted December 19, 2015. Date of publication January 12, 2016; date of current version August 12, 2016. Recommended by Technical Editor J.-Y. (James) Chang. This work was supported in part by Instrument Development Major Program of National Natural Science of China under Grant 61327811, International S&T Cooperation Program of China under Grant 2014DFA70470, National Natural Science of China under Grant 61174087, Grant 61233010 and Grant 61528304, and Jiangsu Natural Science Founds for Distinguished Young Scholar under Grant BK2012005, and the Shanghai Municipal Science and Technology Commission Project under Grant 14JC1491500.

Y. Wang, J. Zhu, J. Luo, M. Liu, and S. Xie are with the School of Mechatronic Engineering and Automation, Shanghai University, Shanghai 200072, China (e-mail: 15106201197@163.com; juhui627@gmail.com; luojun@shu.edu.cn; mliu@shu.edu.cn; srxie@shu.edu.cn).

M. Pang is with the College of Automation, Harbin Engineering University, Harbin 150001, China (e-mail: guanglongriyue@163.com).

C. Zhou and M. Tan are with the Chinese Academy of Sciences, Institute of Automation, Beijing 100190, China (e-mail: chao.zhou@ia.ac.cn; min.tan@ia.ac.cn).

J. Ge and Y. Sun are with the Department of Mechanical and Industrial Engineering, University of Toronto, Toronto ON M5S 3G8, Canada (e-mail: geji@ime.ac.cn; sun@mie.utoronto.ca).

L. Sun is with the Research Center of Robotics and Micro Systems & Collaborative Innovation Center of Suzhou Nano Science and Technology, Soochow University, Suzhou 215021, China (e-mail: lnsun@hit.edu.cn).

C. Ru is with the Research Center of Robotics and Micro Systems & Collaborative Innovation Center of Suzhou Nano Science and Technology, Soochow University, Suzhou 215021, China, and also with the College of Automation, Harbin Engineering University, Harbin 150001, China (e-mail: rchhai@gmail.com).

Color versions of one or more of the figures in this paper are available online at http://ieeexplore.ieee.org.

Digital Object Identifier 10.1109/TMECH.2016.2517102

I. Introduction

POSITIONING stages with nanometer resolutions are required in many micro-nanotechnology applications (e.g., nanometer measurement and semiconductor manufacturing) [1]–[3]. In particular, piezoelectric actuators are widely used for the construction of precision positioning stages because of their inherent subnanometer resolution, high frequency, high energy density, and no backlash [4]. In order to achieve a relatively large travel range (e.g., tens of millimeters), techniques have been developed to accumulate or amplify deformations produced by piezoelectric actuators while ensuring a high resolution [5], [6]. These transscale techniques enabled designs include macro and micro hybrid drive stages, inchworm drive stages, stick-slip drive stages, and parallel kinematic micropositioning stages [7], [8].

Dimensions of hybrid drive stages are large, making them often unsuitable for use in space limited applications. Inchworm stages require relatively complex control mechanisms. Dong *et al*. reported a dual-stage actuation system consisting of a voice coil motor for coarse positioning and a piezoelectric stack actuator to produce fine motion with a positioning accuracy of $\pm$20 nm [9]. Liu *et al*. utilized the integration of a traditional ball-screw stage and a three-axis piezoelectric stage for transscale positioning [10]. In the design, the traditional ball-screw stage consisting of two guide-ways and a ball-screw for each axis was used for long travel (300 mm $\times$ 300 mm), and the piezoelectric stage consisting of three piezoelectric actuators and four translation-rotation mechanisms was used to achieve linear and angular motions. The accuracies were 10 nm and 0.1°, respectively. Li *et al*. developed a decoupled piezo-driven *XYZ* parallel positioning stage [11]. The stage has identical dynamic behavior along the three axes with an accuracy of 0.1 μm. Gao *et al*. reported a two-axis positioning stage by combining lever and parallel mechanisms [12]. The piezo-driven positioning stage has a resolution of 20 and 18 nm and travel ranges of 45 and 40 μm along the two axes.

Stick-slip enables transscale precision positioning with the advantages of high resolution and small size. A systematic investigation and performance comparisons of different stick-slip and slip-slip modes of operation were previously discussed in Hunstig's research [13]. Criteria such as steady-state velocity, smoothness of motion, and start-up time were used for comparisons. Shimizu *et al*. utilized the stick-slip principle and piezoelectric actuators to develop an *XY* positioning stage [14]. The stage was capable of moving over a range of $\pm$1 mm in both directions at a travel speed of 5 mm/s. The piezoelectric

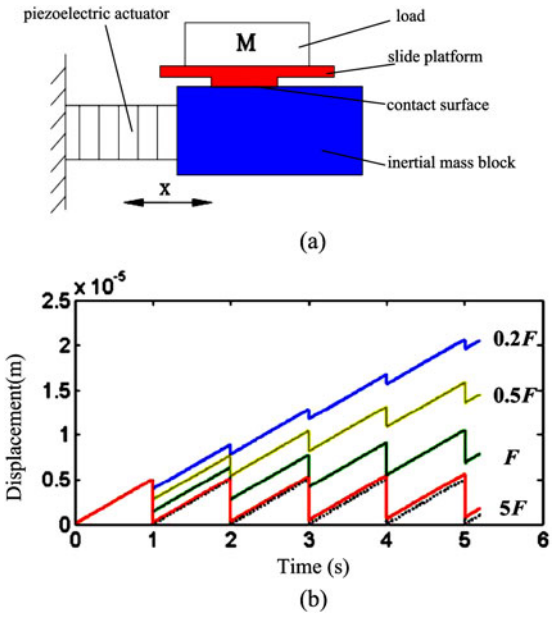

Fig. 1. (a) Schematic illustration of stick-slip drive. (b) Simulation of stage displacements versus varying loads. In simulation, 1 $F = 0.3$ Newton.

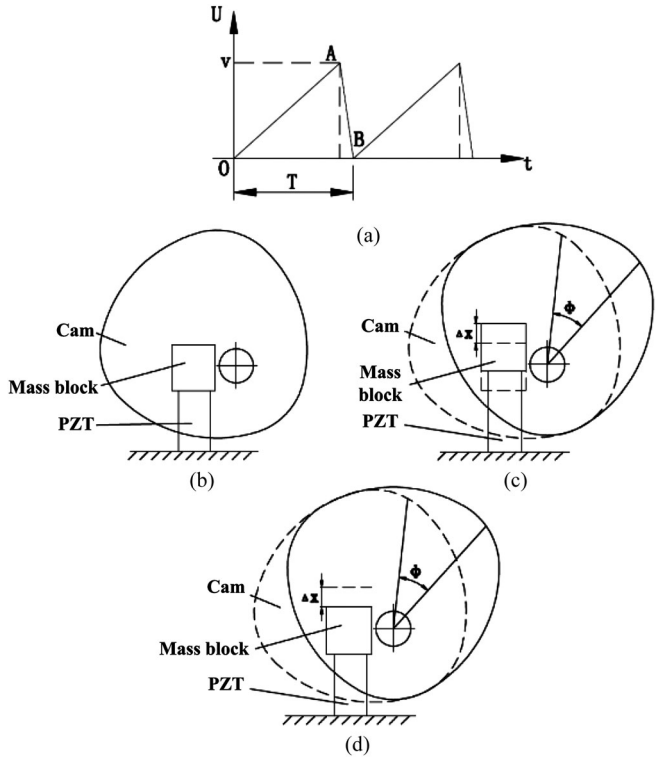

Fig. 2. (a) Sawtooth driving signal. (b)–(d) Motion states of the stick-slip platform: initial state; state in the OA phase; state in the AB phase.

stick-slip positioning stage developed by Rakotondrabe *et al.* had a step resolution of 70 nm, a maximal speed of 1.8 μm/s, and an angular resolution of 0.001° [15].

Stick-slip drive stages have high requirements in machining precision and assembly accuracy. Hence, high precision steering mechanisms are typically used to ensure motion straightness. Additionally, controlling/adjusting friction parameters of stick-slip interfaces can be difficult. Stick-slip drive is based on the friction between interacting surfaces to transfer kinetic energy. The essence is to use the maximum static friction and sliding friction to control the movement of the driven object [16], [17]. As illustrated in Fig. 1(a), the slide platform is in direct contact with the inertial mass block driven by the piezoelectric actuator. The slide platform is moved under the friction force between the contact surfaces. However, the positive pressure between the slide platform and the inertial mass block changes when the load to drive varies. As a result, the friction force is affected which undesirably leads to inconsistent displacements.

To explain this effect further, simulation results when the load on the platform changes and other parameters remain constant was shown in Fig. 1(b). As the load becomes higher (from 0.2 to 5 F where 1F = 0.3 N), the displacement of each step decreases, and the amount of slide backhaul increases. Sufficiently high, a load can make net displacement of the stage almost zero [e.g., under 5 F in Fig. 1(b)]. In order to overcome the effect of load variations on positioning performance and to adjust the preload between the platform and the inertial mass block, Chu *et al.* adopted two precision cylindrical rails to support the platform [1]. However, in practice, it is difficult to control preload via adjusting the many spring screws. Zhong *et al.* utilized an elastic element to support the platform and adjusted preload by deforming the elastic element through a single screw [18]. However, when the load changes or the load is unbalanced, the elastic element also generates a relative deformation which directly affects the friction force.

This paper presents a piezoelectric transscale stick-slip positioning stage that uses a form-closed cam mechanism. High accuracy and large travel range were achieved. Dynamic and vibration models of the stage are established. Kinematic performance of the constructed stage was tested. A trade-off solution is given to the interaction constraints among positioning accuracy, travel range, and stage dimension. A nut and a Belleville spring are utilized to adjust the positive pressure of the friction interface. Two cross roll guide rails are used to guide the platform motion. Hence, the effect of load variations on friction parameters and positioning performance is reduced.

II. Design of Stick-Slip Stage

A. Principle of Motion

Fig. 2 illustrates the moving principle of the stick-slip platform with a cam mechanism with a sawtooth driving signal. The cam is driven by the friction mass block in the form of "stick" when the driving signal increases gradually. Contact force in this phase is the maximum static holding force, as shown in Fig. 2(c), where the mass block moves Δx along the driving direction while the cam rotates by Φ. As the driving signal suddenly decreases, the mass block swiftly returns to the original position in the form of "slip" while the cam maintains static because the inertial force is larger than the maximum static friction force between the mass block and the cam, as shown in Fig. 2(d). Consequently, the cam moves forward one unit step

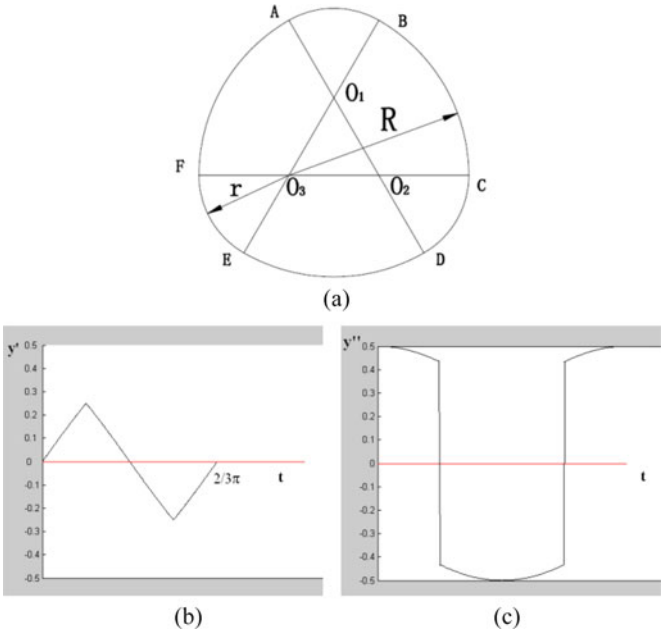

Fig. 3. (a) Arc-triangular-shaped positive-drive cam structure used in this work. (b) Velocity of the follower's motion. (c) Acceleration of the follower's motion.

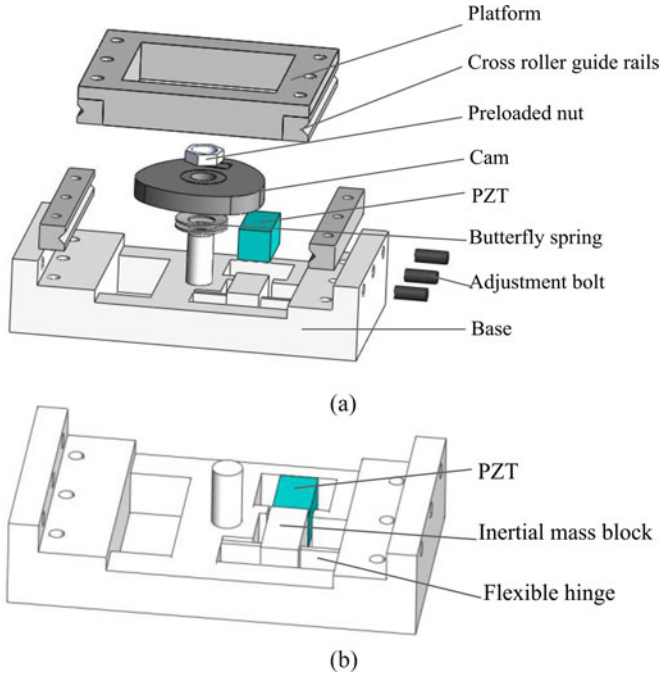

Fig. 4. (a) Components of the positioning stage. (b) Structure of the driving unit.

displacement when the mass block returns to its initial position. As the sawtooth driving voltage increases and decreases cyclically, the stick and slip of the stage occurs iteratively, and the cam is driven step by step. In the closed form with the cam, the platform demonstrates a linear movement through an extended travel range.

According to the applied driving voltage waveform, the positioning stage can operate in either a stepping mode or a scanning mode. In the stepping mode, the stage is driven through an extended displacement range by exploiting the stick-slip friction effect between the mass block and the cam. In the scanning mode, as shown in Fig. 2(c), the stage works as an elastic deformation-type linear device. The platform moves according to the deformation of the piezoelectric actuator in high precision and micrometer range as the driving voltage changes slowly.

In a cam device, the movement of the follower is usually continuous or intermittent reciprocating or oscillating. In this paper, we use an arc-triangular-shaped positive-drive cam structure with the rotation center of the cam coinciding with its geometric center. Therefore, there is no centrifugal force or pressure angle in the cam device. As shown in Fig. 3(a), O1, O2, and O3 are the center of each arc, and R and r are the circular radii. According to the geometric characteristics of the structure, in one rotating cycle of the cam, the follower completes three cycles of motion. The motion equation is

$$y(\omega t) = \begin{cases} R - c\cos(\omega t) & 0 \le \omega t \le \frac{\pi}{6} \\ eR + c\cos(\frac{\pi}{3} - \omega t) & \frac{\pi}{6} < \omega t \le \frac{\pi}{2} \\ R - c\cos(\frac{2\pi}{3} - \omega t) & \frac{\pi}{2} < \omega t \le \frac{2\pi}{3} \end{cases} \quad (1)$$

where ω is the angular velocity, e is the round rate describing the approximation between the arc-triangular-shape and the circular shape, $e = r/R$, and $c = R(1-e)/\sqrt{3}$. Accordingly, the stroke of the follower is

$$h = (R - r)(\frac{2}{\sqrt{3}} - 1). \quad (2)$$

According to (1), Fig. 3(b), (c) shows speed and acceleration of the platform. The velocity of the follower is a continuous function without self-locking or rigid impact.

B. Stage Design

Fig. 4 schematically shows the structure of the positioning stage consisting of a driving unit and a moving unit. The driving unit includes a piezoelectric actuator, flexible hinges, and mass block. The moving unit includes a form-closed cam, platform, and two cross roller guide rails. The driving unit is separated from the moving unit; hence, the influence of the load exerted on the platform to the positive pressure is reduced. In the driving unit as shown in Fig. 4(b), the application of a driving voltage to the piezoelectric actuator produces displacements of the inertial mass block. The flexure hinges serve as a link between the inertial mass and the base. The flexure hinges have the advantages of no friction, no backlash, and high response [19]–[21].

In the moving unit, friction of the contact surface between the cam and the inertial mass block produces driving forces. The butterfly springs and the adjusting bolts provide the stage with adjustable preload. The cam matches with the slide platform in a closed form, and the platform is connected to the base by cross roller guide rails. Parallel cross roller guide rails are used in this design to achieve precise linear displacements of the platform and restrict angular deviations. Additionally, because of their high stiffness, the cross roller guide rails are able to tolerate vertical loads. Hence, load variations have little effect on the positioning performance of the stage.

C. Analysis and Simulation

Analysis was conducted to confirm that the flexible hinges have sufficient flexibility to produce designed ranges of deformation and stress distribution when supplied with an input displacement by the piezoelectric actuator [22]–[27]. The middle mass block shown in Fig. 4(b) can be considered as a rigid body, since its size is much larger than the thickness of the hinge plate.

According to free vibration without damping, the stage can be simplified as a particle and a spring system. As the thickness of the flexible hinge beam is small, shear deformation and the cross-sectional moment of inertia around the neutral axis can be ignored. The hinge can be modeled as a Bernoulli–Euler beam

$$\rho A\frac{\partial^2 w(x,t)}{\partial t^2}+EI\frac{\partial^4 w(x,t)}{\partial x^4}=f(x,t)-\frac{\partial m(x,t)}{\partial x} \quad (3)$$

where ρ, A, E, I are respectively density, cross-sectional area, elastic modulus, and the moment of inertia; w is the transverse displacement; f is the lateral force on unit length; and m is the outer torque on unit length. When the initial condition is one tip fixed and the other being free, natural frequency of the flexible hinge is

$$\omega=\frac{1}{2\pi}\sqrt{\frac{k}{m}}=\frac{1}{4\pi}\sqrt{\frac{Ebh^3}{ml^3}}. \quad (4)$$

Finite element simulation was conducted using ANSYS. The ten-node Solid 92 tetrahedron element was used. Grid refinement was conducted on the hinge area to avoid local stress concentration. Material was specified to be 7075-T651 Aluminum (Young's modulus value: 71 × 109 N/m2; Poisson's ratio: 0.33). The flexible hinge was set to be 0.6 mm wide and 7 mm long. The overall dimensions of the stage in simulation were 51 mm × 30 mm × 11 mm. With an input displacement of 20 μm, stress diagram of the flexible hinge is shown in Fig. 5(a). Maximum stress in the root of the hinge is approximately 96 MPa while the yield stress of the material is 231–308 MPa. The size of the middle mass block is much larger than the thickness of the hinge in the moving direction. Simulation [see Fig. 5(a)] confirms that the deformation of the mass block itself is order of magnitude lower than deformations of the PZT and flexible hinge. Displacements of a number of key nodes on the surface of the inertial mass block were also analyzed and summarized in Fig. 5(b). In addition, the overall displacement error μ was calculated by dividing the maximum error by the theoretical value, $\mu=\frac{20-19.88}{20}\times 100\%=0.6\%$.

Fig. 5(c) shows with a driving force of 35 N, the displacement of the stage is 23 μm. Natural frequency and stiffness of the flexible hinge were calculated and simulated in FEA (natural frequency: 6.741 kHz from calculation versus 7.314 kHz from FEA; stiffness: 1.21 N/μm from calculation versus 1.52 N/μm from FEA). Cam is used to translate the driving force between the inertial mass block and the platform through stick-slip. Instead of using dynamics equations, FEM analysis was also used to study the dynamic characteristics of the cam. Fig. 5(d) shows that the natural frequency of the designed cam is 28 kHz, exceeding the frequency of the piezoelectric driving signal of about 1.5 Hz. In addition, as shown in Fig. 5(a), when a driving force

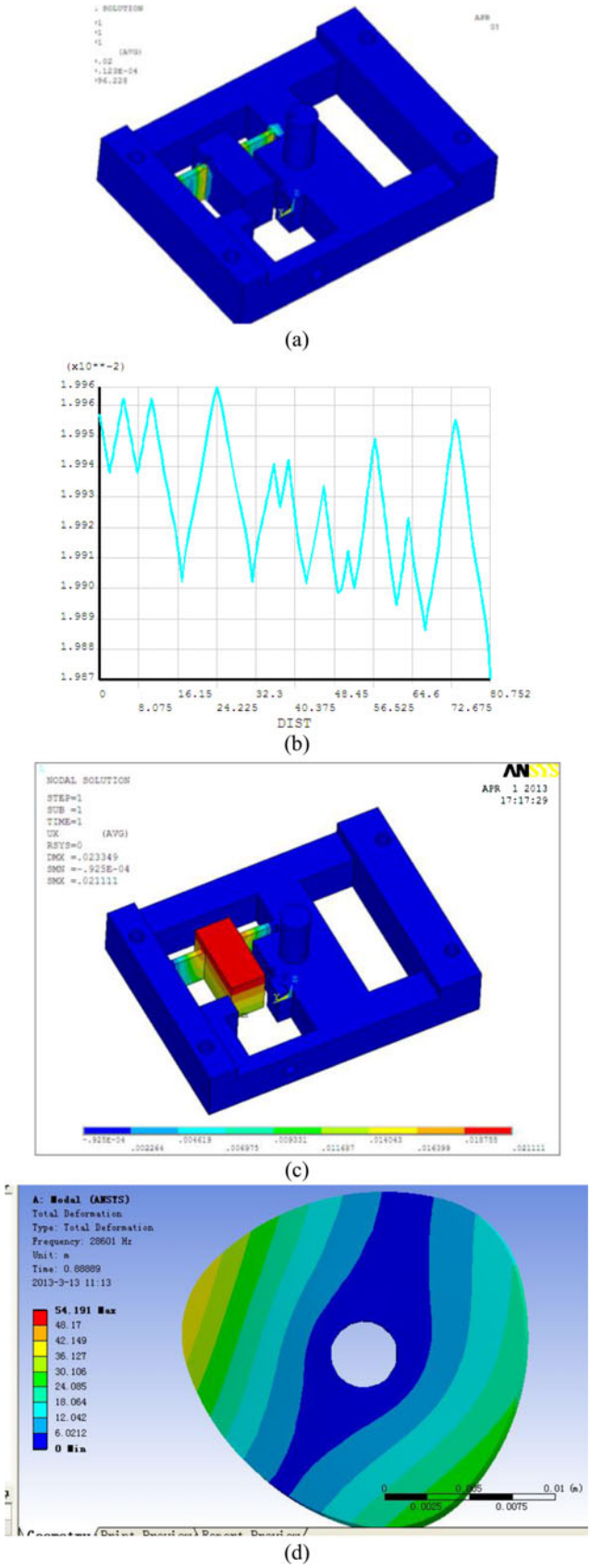

Fig. 5. Finite element simulation results. (a) Stress on the flexible hinge. (b) Summary of displacements on key nodes. (c) Displacement with a driving force of 35 N. (d) FEA modeling of the cam.

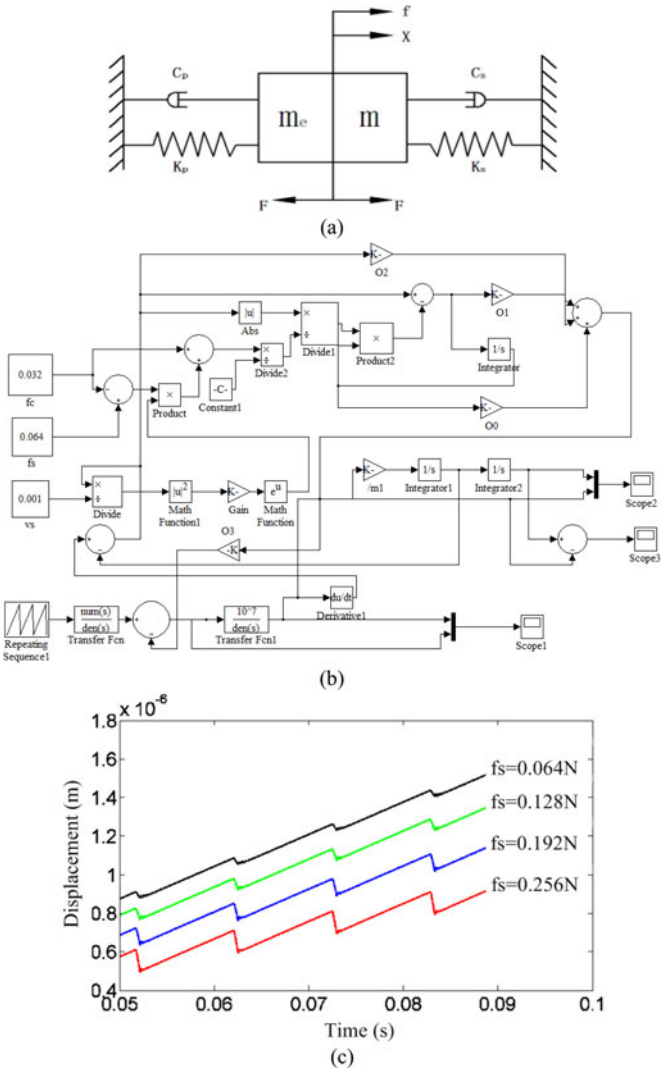

Fig. 6. System dynamic modeling. (a) Simplified model of the driving system. (b) Simulation model used in MATLAB. (c) The influence of maximal static friction force on the displacement produced by the system.

is applied on the driving surface, there exists shear stress on the flexible hinge. Furthermore, simulation [see Fig. 5(c)] reveals that the shear deformation is approximately 3 μm when the driving displacement is 23 μm, which can affect the output displacement of the stage. Therefore, a symmetrical hinge structure was adopted to reduce the influence of shear deformation and reduce this influence. In addition, in stage assembly, PZT was set as parallel as possible to the cross section of the flexible hinge.

The dynamic model of the driving system can be simplified as two spring-damper systems connected in series, as shown in Fig. 6(a). In the driving phase, the PZT was simulated as an electricity model and a mechanical model which translate the driving signal into displacement. Together with the mechanical model of the flexible hinge, the displacement signal after differentiation was then translated into the speed of the mass block. Based on the LuGre friction model, the speed and displacement of the cam were obtained. The simulation model is shown in Fig. 6(b). The MATLAB simulation was used to analyze the

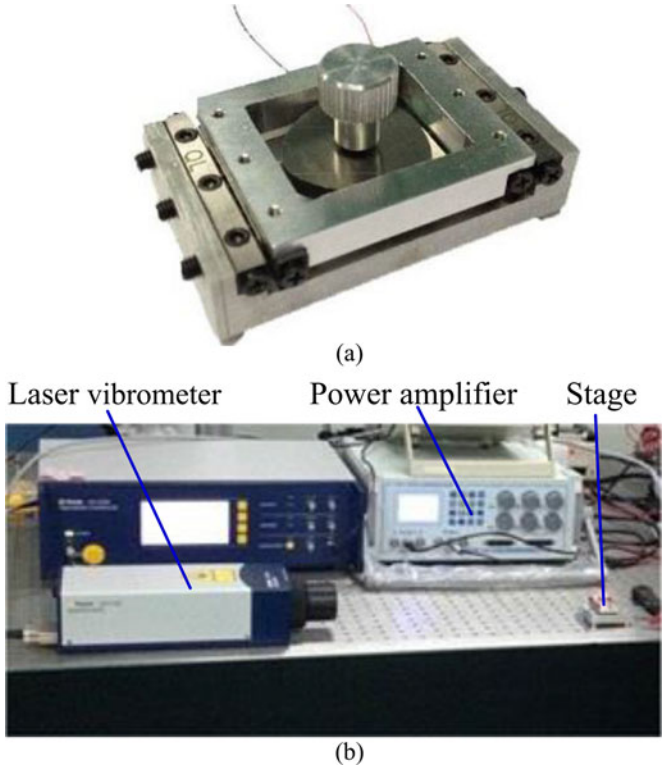

Fig. 7. (a) Constructed positioning stage. (b) Measurement setup.

effect of key parameters and guide the design of the platform. In the simulation model, input driving signals are translated into displacements as the output. As shown in Fig. 1(b), when the pressure between the stick-slip contact surfaces increases, the sliding displacement between the platform and the inertial mass block decreases, which impacts the displacement output of the platform. In the meanwhile, the maximal static friction force of the contacting surfaces changes, resulting in changes of the viscous force between the platform and the inertial mass block. Fig. 6(c) shows that when the maximal static friction force increases, the displacement of the platform increases accordingly in the sliding phase, and the step displacement decreases. Thus, in the platform design, the maximal static friction force of the contact surface and the uniformity of the contact surface should be minimized in order to produce the desired displacement of the platform.

III. Experimental Results and Discussion

A. Stage Construction and Measurement Setup

The stage, as shown in Fig. 7(a), was constructed using electro-discharge machining with a machining resolution better than 0.5 mm. Care was taken to ensure the smoothness of the contact surface where the piezoelectric actuator was subsequently installed. The material of the base and the platform is AL7075, and the material of the cam is 40 Cr. The overall dimensions of the finished stage are 50 mm $\times$ 30 mm $\times$ 11 mm. The piezoelectric actuator measures 5 mm $\times$ 5 mm $\times$ 10 mm, producing a maximum displacement of 10 μm and generating a force of 900 N at 150 V.

In the experimental setup [see Fig. 7(b)], a PC equipped with an NI PCI-6221 DAQ card was used to generate signals (e.g., sawtooth). A power amplifier (BOSHI) amplified the signals to drive the piezoelectric actuator. Displacement of the positioning stage was measured by a noncontact laser interferometer (POLYTEC OFV3001). The setup was placed on a vibration isolation table.

B. Measurement Results

The stage has a bandwidth of up to 140 Hz. Data shown in Fig. 8(a) were measured when a sawtooth voltage (frequency: 1.54 Hz) was amplified to a magnitude of 80 V and then supplied to the piezoelectric actuator. In the rising phase of the voltage, the displacement of the platform is linear with respect to the voltage. In the rapid declining phase, the platform has a short reverse. Net displacement of a unit step is 2.1 μm. Fig. 8(b) shows the resulting displacements from applying a sawtooth voltage of 0.8 V, which is the minimum voltage with which the stage generates measurable displacements. The measured results show that the average step displacement in a single period is 0.0699 μm. Since there are 60 driving pulses within one period, the average value of 1.15 nm was taken as the minimum displacement of the platform.

To quantify precision for each voltage magnitude, the average value of displacements in five cycles was taken and the test was repeated for 15 times. The average value of the 15 step displacements was taken as the nominal displacement under that particular voltage. Fig. 8(c) summarizes the precision test results.

When the driving voltage was increased from 40 to 100 V in steps of 10 V [see Fig. 8(d)], the measurement results show that as voltages increase, the positioning error becomes larger. At the driving voltage of 40 V, positioning accuracy is 27 nm. It can be seen that with the increase of the driving voltage, the step displacement of the platform also increases. In the meanwhile, as voltages increase, displacement fluctuations also become larger, which are attributed to the inherent creep characteristics of piezoelectric actuators.

In this design, the cam mechanism separates the driving unit from the moving unit. Two cross roller guide rails with high stiffness are utilized to drive the load exerted on the platform. The influence of the load on the platform on the positive pressure between the cam and the inertial mass block is reduced as the cam remains still when the load on the platform changes. In experiments, we placed weights on the platform from 10 to 150 g and applied the driving voltage at 80 V with 52 ms step time.

Fig. 9 shows the step displacements under different loads. When the load was increased from 20 to 100 g, the step displacement decreased from 2.24 to 2.10 μm. This result confirms that when the load was increased four times, the step displacement of the stage was reduced only by less than 6.3%. In this design, the cam is driven by an inertial mass block which is moved by the PZT. The cam matches with the slide platform in a closed form, and the platform moves along with the rotation of the cam. Because an arc-triangular-shaped positive-drive cam structure was used, the output displacement of the platform was not completely linear. In addition, as the inertia of the platform

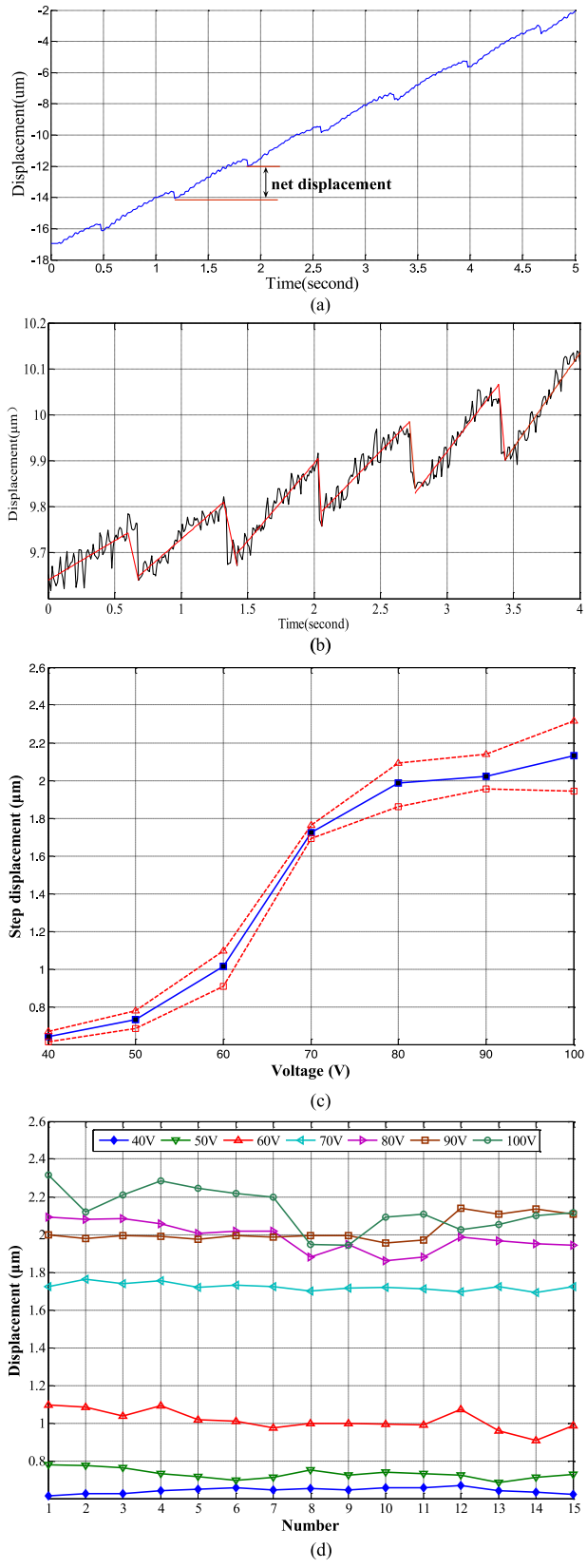

Fig. 8. (a) Displacements under sawtooth driving signal (1.85 Hz; 80 V). (b) Measurement of minimum displacement. (c) Measurement of motion precision: (△) upper deviation; (□) lower deviation; (—) nominal displacement. (d) Step displacements of the platform under different driving voltages.

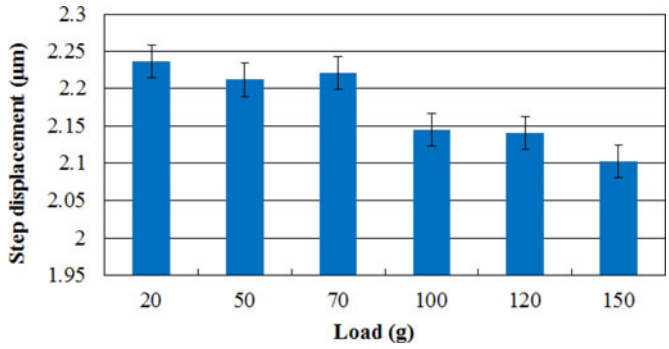

Fig. 9. Step displacements measured under different loads. Measurement was made 15 times under each load condition.

increases with increased loads, more transmission energy is consumed, resulting in the reduction of step displacements.

In contrast, in conventional stick-slip designs without using a cam mechanism [see Fig. 1(b)], the step displacement would decrease by approximately 80% when the load to drive becomes five times. Hence, this design is effective in mitigating the influence from load variations on contact friction force and positioning performance.

C. Discussion

In the stepping mode, the stage has an extended travel range by exploiting the stick-slip friction effect between the mass block and the cam. The driving speed depends on the amplitude and frequency of the driving voltage. In the scanning mode, the stage acts as a linear displacement device through displacements in the micrometer range [28], [29]. Results shown in Figs. 1(b) and 8(a) confirm that the simulation result is in agreement with experimental results. In the rising phase of the actuation voltage, the displacement of the platform is linear with respect to the actuation voltage. In the rapid declining phase, the platform has a short reverse. In addition, results shown in Figs. 1(b) and 9 demonstrate that the designed stage is capable of reducing the influence of the load on step displacements. However, because of machining and assembly imperfections, slight differences of the net displacements of a unit step exist between the simulation and experimental results.

There are several limitations in the present design, which will be tackled in future work. First, the stage structure contains a rotation device and a transmission mechanism in closed form, which are both in clearance fit transmission. As a result, clearance error has great influence on positioning accuracy. In addition, backlash error exists in the positioning process and also in return movement. To overcome these limitations, adopting high precision bearing and reducing the friction coefficient of the contact surface can potentially reduce transmission errors. Second, parallelism and jump of the mounting surface during assembly can affect the straightness of movement. Third, hysteresis and creep of the piezoelectric actuator affect positioning precision which can be improved via employing control approaches.

IV. Conclusion

This paper described a piezoelectric stage, where a new closed-form cam mechanism is used to separate the driving unit from the moving unit. The design significantly reduces the effect of load variations on positioning performance. Butterfly springs are utilized to adjust the preload on the contact surface, and a pair of cross roller guide rails is used for load driving. Theoretical analysis and numerical modeling were conducted to estimate the static and dynamic performance of the design. Experiment results demonstrate that the stage is capable of producing transscale positioning. In the scanning mode, the minimum resolution of the stage is 1.15 nm. In the stepping mode, the stage travels up to 2 mm with a positioning accuracy of 27 nm. Measurements also confirmed that when the load was increased four times, the step displacement of the stage was reduced only by less than 6.3%, while the step displacement of conventional stick-slip stages would decrease by approximately 80%. This stage design can be useful for applications that involve varying loads to drive while requiring nanometer positioning accuracies.

References

[1] C.-L. Chu and S.-H. Fan, "A novel long-travel piezoelectric-driven linear nanopositioning stage," *Precis. Eng.*, vol. 30, no. 1, pp. 85–95, 2006.

[2] J. Wang, C. Zhu, M. Feng *et al.*, "Thermal error modeling and compensation of long-travel nanopositioning stage," *Int. J. Adv. Manuf. Technol.*, vol. 65, pp. 443–450, 2013.

[3] Y. K. Yong, B. Bhikkaji, and S. O. Reza Reza Moheimani, "Design, modeling, and FPAA-based control of a high-speed atomic force microscope nanopositioner," *IEEE-ASME Trans. Mechatronics*, vol. 18, no. 3, pp. 1060–1071, Jun. 2013.

[4] Y. Li and Q. Xu, "A novel piezoactuated XY stage with parallel, decoupled, and stacked flexure structure for micro-/nanopositioning," *IEEE Trans. Ind. Electron.*, vol. 58, no. 8, pp. 3061–3615, Aug. 2011.

[5] *Microsystems and Micro/Nano-Technology in Medical Applications*. Guadalajara, Mexico: Springer-Verlag, 2002, pp. 236–245.

[6] A. I. Cahyadi and Y. Yamamoto, "Modelling a micro manipulation system with flexure hinge," presented at the IEEE Conf. Robotics, Automation and Mechatronics, Bangkok, Thailand, Dec. 2006, vol. 11, pp. 1–5.

[7] B.W. Zhong, Z. H. Wang, L. G. Chen *et al.*, "Current development of trans-scale precision positioning technology based on the stick-slip effect," *Piezoelectr. Acoustoopt.*, vol. 3, pp. 479–485, 2011.

[8] X. Qingsong, "New flexure parallel-kinematic micropositioning system with large workspace," *IEEE Trans. Robot.*, vol. 28, no. 2, pp. 478–491, Apr. 2012.

[9] W. Dong, J. Tang, and Y. EIDeeb, "Design of a linear-motion dual-stage actuation system for precision control," *Smart Mater. Struct.*, vol. 18, no. 9, p. 095035, 2009.

[10] C. H. Liu, W. Y. Jywe, Y. R. Jeng *et al.*, "Design and control of a long-traveling nano-positioning stage," *Precis. Eng.*, vol. 34, no. 3, pp. 497–506, 2010.

[11] Y. Li and Q. Xu, "A totally decoupled piezo-driven XYZ flexure parallel micropositioning stage for micro/nanomanipulation," *IEEE Trans. Autom. Sci. Eng.*, vol. 8, no. 2, pp. 265–279, Apr. 2011.

[12] P. Gao, H. Tan, and Z. Yuan, "The design and characterization of a piezo-driven ultra-precision stepping positioner," *Meas. Sci. Technol.*, vol. 11, no. 2, pp. N15–N17, 2000.

[13] M. Hunstig, T. Hemsel, and W. Sextro, "Stick-slip and slip-slip operation of piezoelectric inertia drives. Part I: Ideal excitation," *Sens. Actuators A, Phys.*, vol. 200, pp. 90–100, 2013.

[14] Y. Shimizu, Y. Peng, J. Kaneko *et al.*, "Design and construction of the motion mechanism of an XY micro-stage for precision positioning," *Sens. Actuators A, Phys.*, vol. 201, pp. 395–406, 2013.

[15] M. Rakotondrabe, Y. Haddab, and P. Lutz, "Development, modeling, and control of a micro-/nanopositioning 2-DOF stick–slip device," *IEEE/ASME Trans. Mechatronics*, vol. 14, no. 6, pp. 733–745, Dec. 2009.

[16] A. Bergander, J. M. Breguet, C. Schmitt *et al.*, "Micropositioners for microscopy applications based on the stick-slip effect," in *Proc. IEEE Int. Symp. Micromechatron. Human Sci.*, 2000, pp. 213–216.

[17] M. Spiller and Z. Hurák, "Hybrid charge control for stick–slip piezoelectric actuators," *Mechatronics*, vol. 21, no. 1, pp. 100–108, 2011.

[18] B. W. Zhong, L. G. Chen, Z. H. Wang *et al.*, "Movement modeling and testing of a novel trans-scale precision positioning stage based on the stick-slip effect," *Adv. Mater. Res.*, vol. 255, pp. 484–687, 2011.

[19] Y. Li and Q. Xu, "Design and analysis of a totally decoupled flexure-based XY parallel micromanipulator," *IEEE Trans. Robot.*, vol. 25, no. 3, pp. 645–657, Jun. 2009.
[20] X. Zhao, C. Zhang, H. Liu *et al.*, "Analysis of hysteresis-free creep of the stack piezoelectric actuator," *Math. Problems Eng.*, vol. 2013, article 187262, 2013.
[21] Z. M. Zhang, Q. An, and J. W. Li, "Piezoelectric friction–inertia actuator—A critical review and future perspective," *Int. J. Adv. Manuf. Technol.*, vol. 62, nos. 5–8, pp. 669–685, 2012.
[22] C. Edeler, I. Meyer, and S. Fatikow, "Modeling of stick-slip micro-drives," *J. Micro/Nano Mechatron.*, vol. 6, nos. 3/4, pp. 65–87, 2011.
[23] T. Fukuda, M. Nakajima, P. Liu *et al.*, "Nanofabrication, nanoinstrumentation and nanoassembly by nanorobotic manipulation," *Int. J. Robot. Res.*, vol. 28, no. 4, pp. 537–547, 2009.
[24] Y. Li and Q. Xu, "A totally decoupled piezo-driven XYZ flexure parallel micropositioning stage for micro/nanomanipulation," *IEEE Trans. Autom. Sci. Eng.*, vol. 8, no. 2, pp. 265–279, Apr. 2011.
[25] S. Xiao, Y. Li, and X. Zhao, "Design and analysis of a novel flexure-based XY micro-positioning stage driven by electromagnetic actuators," in *Proc. IEEE Int. Conf. Fluids Power Mechatron.*, Aug. 2011, pp. 953–958.
[26] B. Chu, Y. Jin, and C. A. Zhu, "Modeling and simulation of Stick-Slip motion of a position stage," *Appl. Mech. Mater.*, vols. 271/272, pp. 1356–1361, 2013.
[27] A. Socoliuc, R. Bennewitz, E. Gnecco *et al.*, "Transition from stick-slip to continuous sliding in atomic friction: Entering a new regime of ultra-low friction," *Phys. Rev. Lett.*, vol. 92, no. 13, pp. 134301–134303, 2004.
[28] Y. Zhang, W. J. Zhang, J. Hesselbach *et al.*, "Development of a two-degree-of-freedom piezoelectric rotary-linear actuator with high driving force and unlimited linear movement," *Rev. Sci. Instrum.*, vol. 77, no. 3, pp. 035112-1–035112-4, 2006.
[29] M. Rakotondrabe, Y. Haddab, and P. Lutz, "Voltage/frequency proportional control of stick-slip micropositioning systems," *IEEE Trans. Control Syst. Technol.*, vol. 16, no. 6, pp. 1316–1322, Nov. 2008.

Yong Wang received the Master's degree in mechanical engineering from the Soochow University, Suzhou, China, in 2014. He is currently working toward the Doctoral degree at the Mechanical and Automation Engineering Department, Shanghai University, Shanghai, China. His research interests include design and fabrication of miacro-nano electromechanical systems, cross-scale nano-positioning technology.

Junhui Zhu received the Master's degree in mechanical engineering from the Soochow University, Suzhou, China, in 2015. He is currently working toward the Doctoral degree at the Mechanical and Automation Engineering Department, Shanghai University, Shanghai, China. His research interests include design and fabrication of miacro-nano electromechanical systems, long-stroke cross-scale nano-positioning technology.

Ming Pang's photograph and biography not available at the time of publication.

Jun Luo received the B.S. degree in mechanical engineering from Henan Polytechnic University, Jiaozuo, China, in 1994, the M.S. degree in mechanical engineering from Henan Polytechnic University, in 1997, and the Ph.D. degree from the Research Institute of Robotics, Shanghai Jiao Tong University, Shanghai, China, in 2000.

He is currently a Professor with the School of Mechatronic Engineering and Automation, Shanghai University. He is also the Head of Precision Mechanical Engineering Department, Shanghai University, and the Vice Director of Shanghai Municipal Key Laboratory of Robotics. His research areas include robot sensing, sensory feedback, mechatronics, manmachine interfaces, and special robotics.

Shaorong Xie received the B.S. and M.S. degrees in mechanical engineering from Tianjin Polytechnic University, Tianjin, China, in 1995 and 1998, respectively, and the Ph.D. degree in mechanical engineering from the Institute of Intelligent Machines at Tianjin University, Tianjin, China, and the Institute of Robotics and Automatic Information System, Nankai University, Nankai, China, in 2001.

She is currently a Professor with the School of Mechatronic Engineering and Automation, Shanghai University, Shanghai, China. Her research interests include advanced robotics technologies, bionic control mechanisms of eye movements, and image monitoring systems.

Mei Liu's photograph and biography not available at the time of publication.

Lining Sun received the B.S. degree in mechanical engineering, the M.S. and Ph.D. degrees in mechatronics engineering from Harbin Institute of Technology, Harbin, China, in 1985, 1988, and 1993, respectively.

He is currently with the State Key Laboratory of Robotics and Systems, Robotics Institute, Harbin Institute of Technology and the Research Center of Robotics and Micro Systems and Collaborative Innovation Center of Suzhou Nano Science and Technology, Soochow University, Suzhou, China. His research interests include robot control, design of actuators, design and control of high-speed machines, microelectromechanical systems (MEMS) 3-D assembly, MEMS robotic task execution, micromanipulation robots, etc. He has published extensively in journals and conference proceedings and has supervised more than 50 M.S. and Ph.D. students and a number of Postdoctoral Fellows and Research Engineers in these various research areas.

Chao Zhou received the B.S. degree (Hons.) in automation from Southeast University, Nanjing, China, in July 2003, and the Ph.D. degree in control theory and control engineering from the Institute of Automation, Chinese Academy of Sciences, Beijing, China, in 2008.

Since July 2008, he has been an Assistant Professor in the Key Laboratory of Complex Systems and Intelligent Science, Institute of Automation, Chinese Academy of Sciences, where he has been an Associate Professor since October 2011. His current research interests include the motion control of robot, the bio-inspired robotic fish, and embedded system of robot.

Min Tan received the B.E. degree from Tsinghua University, Beijing, China, and the Ph.D. degree in control theory and control engineering from the Institute of Automation, Chinese Academy of Sciences, Beijing, in 1986 and 1990, respectively.

He is currently a Professor in the State Key Laboratory of Management and Control for Complex Systems, Institute of Automation, Chinese Academy of Sciences. His research interests include advanced robot control, biomimetic robot, multirobot system.

Ji Ge's photograph and biography not available at the time of publication.

Yu Sun (S'01–M'03–SM'07) received the B.S. degree in electrical engineering from the Dalian University of Technology, Dalian, China, in 1996, the M.S. degree from the Institute of Automation, Chinese Academy of Sciences, Beijing, China, in 1999, and the M.S. degree in electrical engineering and the Ph.D. degree in mechanical engineering from the University of Minnesota, Minneapolis, MN, USA, in 2001 and 2003, respectively.

He is currently a Professor with the Department of Mechanical and Industrial Engineering and also with the Institute of Biomaterials and Biomedical Engineering and the Department of Electrical and Computer Engineering, University of Toronto, Toronto, ON, Canada. He is the Canada Research Chair in Micro and Nano Engineering Systems. His research areas include the design and fabrication of M/NEMS devices, micronanorobotic manipulation, and the manipulation and characterization of cells, biomolecules, and nanomaterials.

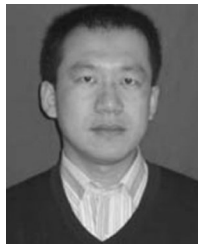

Changhai Ru (M'07) received the Ph.D. degree in mechatronics engineering from the Harbin Institute of Technology, Harbin, China, in 2005.

He was a Postdoctoral Fellow in the Department of Mechanical and Industrial Engineering, University of Toronto, Toronto, ON, Canada. He is currently a Professor with the Research Center of Robotics and Micro Systems & Collaborative Innovation Center of Suzhou Nano Science and Technology, Soochow University, Suzhou, China, and College of Automation, Harbin Engineering University, Harbin, China. His research interests include micro/nanomanipulation, nanopositioning technologies, and solid-state actuators' driving and control methods.